TANWEER ALAM
and
BIRENDRA KUMAR

Effect of coating thickness on SI engine performance

Present work is intended to investigate the stress and temperature distribution for a partially coated spark ignition (SI) engine piston. For comparison purpose analysis was also made on uncoated piston and results were compared to the temperature and stress distribution obtained from the application of different coating thickness and width on the piston. It is found that increase in coating surface temperature with coating thickness is in a decreasing rate. From the analysis of bond coat surface, it is found that with the increase in coating thickness decrease in normal stress is steady while rise of maximum shear stress is in decreasing rate.

Keywords: *Ceramic coating; spalling; bond coat; piston; coating thickness, crevices.*

Introduction

To improve the service performance of internal combustion engine components, thermal barrier coating (TBC) is one of the means widely in use [1-5]. TBCs were not only used to reduce in cylinder heat rejection and thermal fatigue protection of underlying metallic surfaces for engines, but also to reduce engine emission [6-8]. For TBC, monolithic ceramic such as zirconia having high thermal insulating property along with the capability to stand against high temperature gradients and in some cases, higher value of temperature differences are used. The bond coat is an intermetallic alloy that provides oxidation resistance at high temperatures and aids in the adhesion of the TBC to the substrate [10-11]. The sole purpose of TBCs applications on the piston surface are the reduction of heat flux into the piston, protection of the piston from thermal stresses and corrosive attacks from fuel contaminants and reducing the emissions [4-5, 21-22]. Due to TBC, combustion chamber rejects low heat from thermally insulated component and hence amount of available energy caused the increase in cylinder work and the amount of energy carried by the exhaust gases, which could also be utilized [8, 14].

Messrs. Tanweer Alam, Assistant Professor and Birendra Kumar, Department of Mining Machinery Engineering, IIT/ISM, Dhanbad, Jharkhand, India 826 004. e-mail: tanweer.amu@gmail.com and bikr285@gmail.com

Several researchers have examined the application of TBCs in SI engines and reported about the improved performance and emission [15, 17, 22]. However instead of full coating, partial ceramic coating on SI engine pistons could improve the performance, fuel economy, and exhaust emissions, the degree of insulation is an important factor that needs to be investigated for knock free performance. The sole purpose of partial TBC application is to increase the unburned charge oxidation near the entrance of the clearance between the piston and liner during compression and early part of the expansion stroke [5-17]. The main source of the cold start HC emission from SI gasoline engines is crevice, flame quenching region. For TBC, the top surface near the crevice is chosen in order to reduce the knocking possibility. It was mentioned by the researchers that the temperature increase results in an increase in air fuel mixture temperature in crevice section and thus unburned charge oxidation near the entrance of the clearance between the piston and liner increased. The rise in temperature also caused the increase in mixture temperature in the wall quenching region, and hence a significant decrease in HC emissions arisen from wall quenching was obtained. TBC significantly improves combustion efficiency and HC emissions in comparison with the standard piston engine [15, 17].

Problem formulation

The variation in coating thickness affects the combustion temperature, stress distribution and temperature gradient in the coating and the interfacial stresses. Thermal shocks produced due to temperature difference between the top coat and substrate are one of the reasons of internal stresses between aluminum alloy and ceramic coating. Application of bond coat in between reduces the chances of occurrence of internal stresses. The elastic modulus, thermal expansion coefficient and thermal conductivity are few parameters affecting the thermal shock resistance of a ceramic coating. Crack nucleation and its propagation in parallel direction to the ceramic bond coat interface (horizontal crack) restricts the life of TBC and leads to the coating delamination. Spalling of top ceramic coat from bond coat is also one of the reasons of TBC failure. Overall performance of coatings and spalling of the coating are influenced by the other factors also but oxidation and thermal mismatch are the two main features affecting the life of the coating system [18-19]. For controlling of thermal stresses and deformations within the acceptable regions necessitates the calculation of piston temperature distribution.

Methodology

The present work is focused on the reduction of cold start HC emission during idle condition and to enhance the performance characteristics for wide open throttle condition. For this purpose, the top surface of the piston near the crevice was taken as partially coated with thermal barrier coating (TBC). Low thermal conductive ceramic material, partially stabilized zirconia, was chosen to coat the outer region of the piston top surface. In order to have constant volume combustion chamber, the coating layer of certain thickness and width was removed from the standard piston top surface circumferentially. Further a 0.15 mm of NiCrAl bond coat and various thicknesses of ceramic $MgZrO_3$ layers were assumed to be coated on the annular section. Original partially coated piston, schematic representation of the half part of the model, coating and bond coat constituents are given in Fig. 1a–b.

In the present work, thermal and structural analysis was made for steady state condition to find the thermal barrier coating effect on stress and temperature distribution for the crevice and regions of wall quenching petrol based pistons. Numerical analysis based on finite element method (FEM) was made. Focus was made to obtain the optimum value of thickness in order to reduce coating separation, interfacial stress and surface stress. Table 1 represents the value of thickness and width taken for analysis purpose. A single cylinder SI engine piston was considered for analysis purpose. Table 2 shows the specification of engine piston used for analysis purpose. For FEM analysis half part of model was considered in Fig.1a-b. Fig.1b indicates the interfaces for different types of bindings. The model includes the base metal, bond coat and ceramic coating. Piston and rings are made of AlSi alloy and cast iron respectively and materials are considered as elastic and isotropic in nature. Although the materials have different thermos-mechanical characteristics for each directions and coatings have ceramic metal configuration and may not be assumed isotropic. Thermally sprayed ceramic material has layered structures with defect density resulting from successive impingement of a multitude of fully or semi molten particles. For analysis purpose plasma sprayed coating was considered due to having transversely isotropic symmetry. The coating material properties may be different in through thickness and in-plane directions but its behaviour is linear in each direction. The present system was modelled as three distinct layers with clearly defined interface along them. Table 3 shows the thermos-mechanical properties of the piston, rings and the coating material. For thermal barrier coating, stabilized zirconia was considered due to better thermal insulating property, thermal and chemical stability at very low and high temperature applications.

For thermo-mechanical analysis purpose, mechanism of heat transfer is considered as convection. Heat transfer model in the ring land and skirt region was generated using thermal circuit method with the assumption that effect of piston motion on the heat transfer is neglected, rings do not twist, rings and skirt are fully immersed in oil and no cavitation occurs and conductive heat transfer in the oil film is neglected [4]. The model symmetric plane was imposed with symmetric constraints, while adiabatic condition was taken for cutting surfaces of the piston fixed to

Table 1. Dimensions of Partially coated ceramic

Thickness (t_1) of Ceramic coat ($MgZrO_3$) (mm)	Thickness (t_2) of Bond coat (NiCrAl) (mm)	Total coating (mm)	Width (w) of Coating (mm)
0.15 – 1.05	0.15	0.30 - 1.60	8.00
0.25	0.15	0.50	4.20 - 10.20

Table 2. Engine Specification

Bore	53.97 mm
Stroke	51.55 mm
Displacement	233.05 mm^3
Compression ratio	6.8
Power (at 3000 rpm)	4.4 kW
Maximum speed	3300 rpm

Table 3. Properties of piston, rings and ceramic (Matthew and Parker, Kahl (1993))

Material	Young's modulus (GPa)	Poisson's ratio (υ)	Thermal conductivity (W/m °C)	Thermal expansion 10^{-6} (1/°C)	Density (Kg/m^3)	Specific heat (J/kg °C)
Rings	200	0.30	16	10	7300	460
Base metal (AlSi)	69	0.33	155	21	2700	960
Bond coat (NiCrAl)	90	0.27	16.1	12	7870	764
Ceramic ($MgZrO_3$)	46	0.20	0.80	08	5600	650

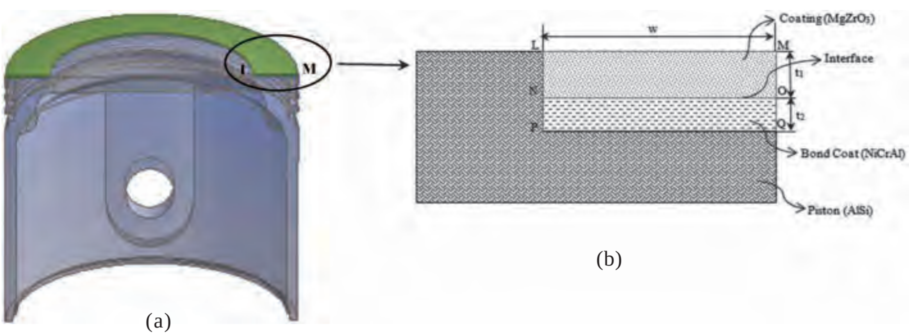

Fig.1(a) Half part of partially coated piston, and (b) Parameters used during analysis the normal direction. The piston was supported by a rigid, motionless gudgeon pin and at the surface of gudgeon pin-hole displacements was set to zero. Engine cycle simulation code for the piston top [21] was used to calculate the local average heat transfer coefficient and gas temperature boundary conditions. The code calculates the heat transfer coefficients having interval of one crank angle degree. These values were assumed to be constant. The piston surface is heated in a point wise-like way at the outlet of the swirl chamber and cooled through contact with cooler components of the combustion chamber. In the study, following correlation, Eq. (1) was used to predict instantaneous heat transfer coefficients [20].

$$H_g = K_1 V_c(t)^{-0.06} P(t)^{0.8} T(t)^{0.4} \left(\bar{S}_p + K_2\right) \qquad \ldots \qquad (1)$$

where $H_g(t)$ is the instantaneous convective heat transfer coefficient (W/m^2.K), $V_c(t)$, $P(t)$ and $T(t)$ are the instantaneous cylinder volume (m^3), pressure (bar) and temperature (K), and S_p are the mean piston speed (m/s), respectively. The value of calibration constants, 'K_1' and 'K_2' are calculated and used as 130 and 1.4. Heat transfer coefficient and temperature values for piston top were taken as cycle averaged values [4]. Boundary conditions for oil-cooled part of the piston were obtained from literature. Fig. 2a-b represents boundary conditions value for heat transfer coefficient and temperatures [21].

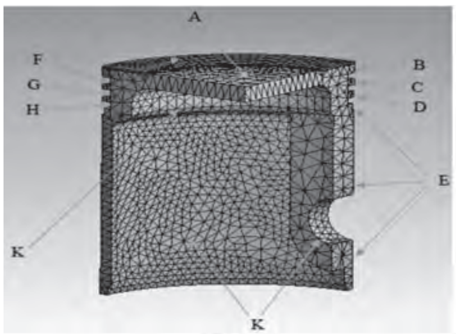

(a)

Region	Heat Transfer Coefficient W/m^2 °C	Temperature (°C)
A	600	650
B	350	500
C	300	180
D	400	170
E	400	110
F	300	200
G	300	180
H	300	170
K	1500	95

(b)

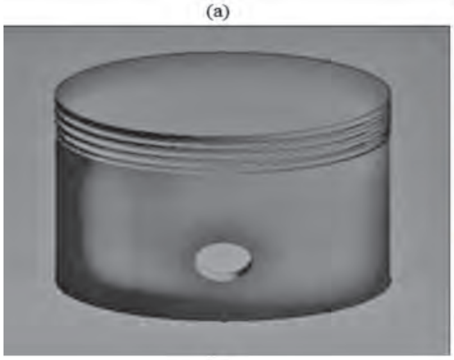

(c)

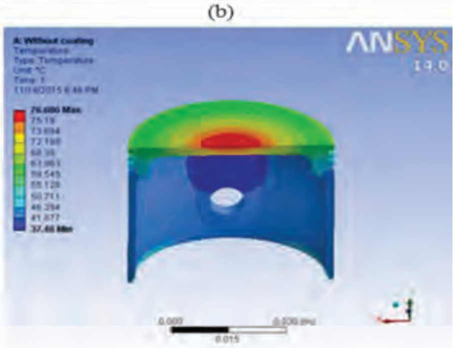

(d)

Fig.2(a) Boundary Conditions of the Piston [10] (b) Heat transfer coefficient and temperature values for different regions (c) Model used for analysis, and (d) Temperature distribution for uncoated piston

Result and discussion

Fig.2c represents model used for analysis purpose whose specification is given in Table 2. Fig.2d shows the temperature distribution on uncoated piston surface. It was observed that maximum temperature occurs at the center of top surface and its value decreases towards the edge and piston skirt. Fig.3a-h shows the temperature distribution on coated piston surface with various coating thicknesses and width. Ceramic coated piston have higher value of temperature due to having relatively low heat transfer coefficient. It was observed that increase in surface temperature for TBC piston is very sharp and percentage of increase in temperature increases with coating thickness as compared to uncoated.

These variations are in conformity with the results obtained for the diesel aluminum alloy and steel piston [3, 5]. It was observed from Fig.3a-h, the surface temperature remains almost same in the uncoated region for increased coated surface width with the same coating thickness. For coating thickness of 0.9 mm the value of temperature is maximum and is 264.7ºC. Top surface temperature variation for uncoated and coated piston with different coating thicknesses were shown in Fig. 4a. It was observed that in uncoated region the slight surface temperature variation is there while for coated region the increase is very sharp and non-linear for all models with different coating thicknesses. From this it can be deduced that there is possibility to reduce cold start hydrocarbon (HC) emission by applying a coating thickness of minimum value up to 0.30 mm. Fig. 4b shows the variation of top surface temperature for uncoated and coated piston for same coating thickness and with different coating width. It was observed that for uncoated region there is no significant change in temperature for all pistons and the temperature variations have the same characteristics up to the border of the coated regions for each coating width.

Fig. 5 shows variation of maximum temperatures with the coating thickness for ceramic coating, bond coat and base metal surfaces. The increase in coating surface temperature was found with the increase in coating thickness for all three cases. The higher rate of increase was found in ceramic coating. The base metal surface than bond coat shows lesser increase rate. For base metal and bond coat material, the temperature curves are

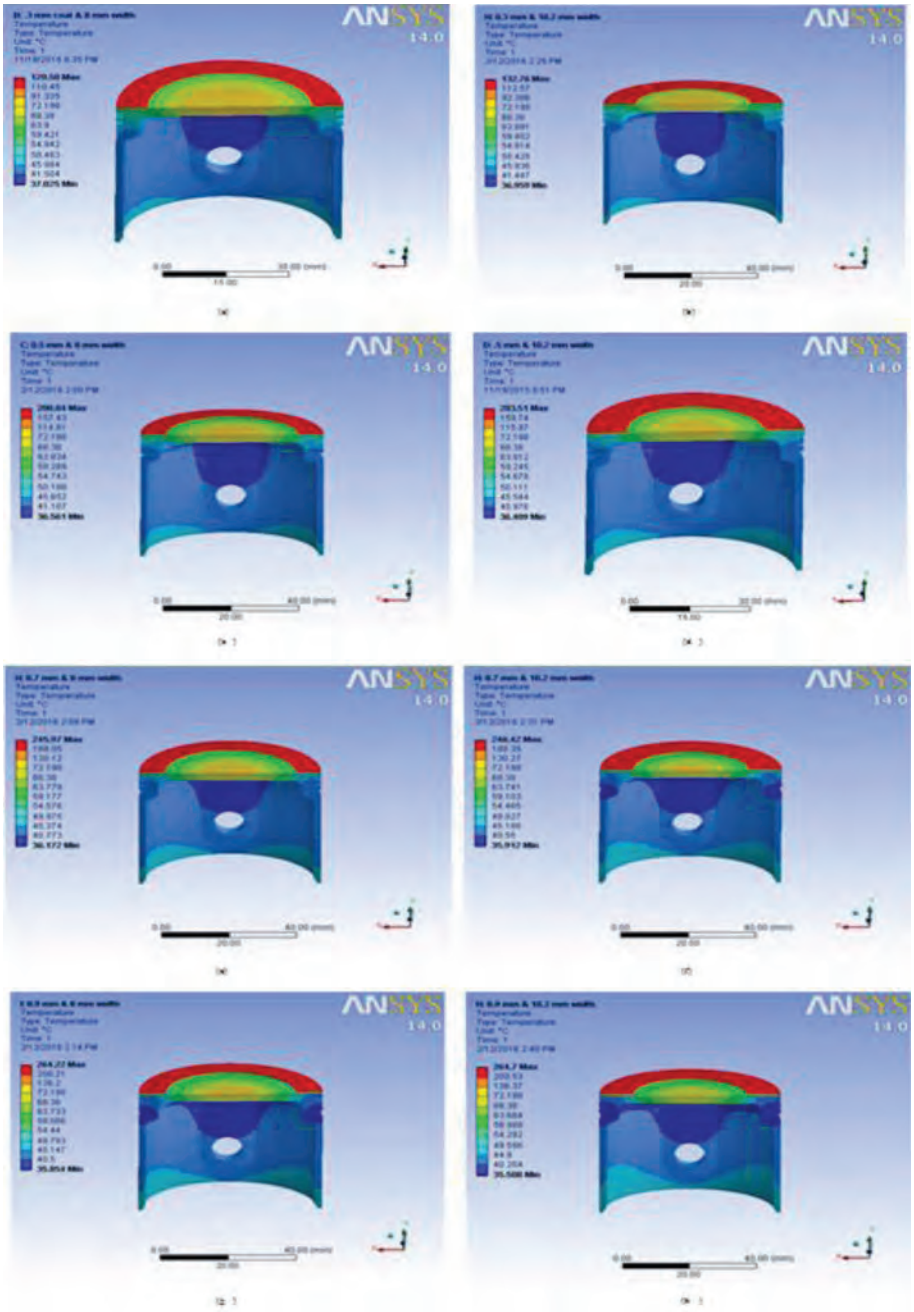

Fig.3

almost parallel with a temperature difference value lesser than 3°C. It is because of higher value of thermal conductivity of bond coat and base material than ceramic coating and hence limited heat transfer into the substrate and bond coat.

Fig. 6 shows the variation of Von Mises stress distribution with radial distance for uncoated and coated piston with different coating thickness. For uncoated piston, normal stress value varies between 6 and 20 MPa. For coating thickness of 0.30 mm, the maximum value of 182 MPa was obtained at the middle of coated region and further decrease in maximum value was observed with the decrease in coating thickness up to 0.9 mm thickness, having minimum value. It can be concluded that optimum value of coating thickness for this particular condition with respect to normal stress is 0.9 mm. One of the researchers (Jesse et. al. (2002)) also observed the same for diesel engine piston, in which maximum stress varies as a function of coating thickness.

Fig.7 shows the variation of Von Mises stress distribution with radial distance for thermal barrier coated pistons having various coating thickness values in the interfacial bond coat surface (Line NO, the ceramic-bond coat interface). The bond coat ceramic coating interface has maximum value of normal stress and further the decrease in value was observed with increase in thickness. Due to higher thermal expansion coefficient value of bond coat material than ceramic coating, the maximum value of stress was observed at the interface between $MgZrO_3$ ceramic coating and NiCrAl bond coat.

Fig.8 shows the variation of shear stress distribution versus radial coating distance for thermal barrier coated piston for the upper bond coat surface (Line PQ, at the bond coat-substrate surface). It was observed that maximum value of shear stress appears at the edge of coated region and changes its direction in the middle of coating. The value of maximum shear stresses increases with the increase in coating thickness and very high values appeared on the inner and outer edges of coated region. Fig. 9 shows the Von Misses stress distributions versus radial coating distance for coated pistons at the bond coat–base metal interface. It was observed that normal stress value is maximum at the edge of coated region and increases with the coating thickness. The coated region inner side normal stress value is higher than outer side and further increase was observed with increase in thickness.

For thermal barrier coated piston, shear stress distribution versus radial coating distance was shown in Fig.10. The value of shear stress increases with the coating thickness and the maximum value was observed at the edge of the coated region. Shear stress is similar to ones on the bond coat

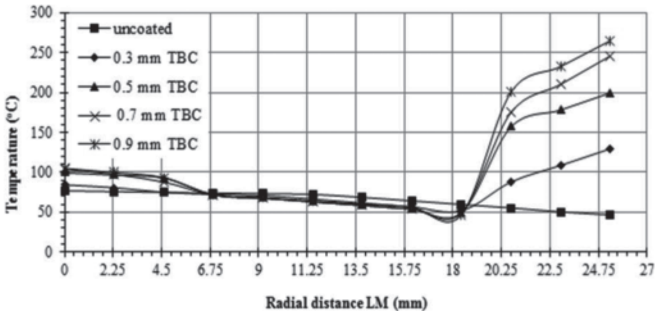

Fig.4(a) Top surface temperature distribution with coating thickness

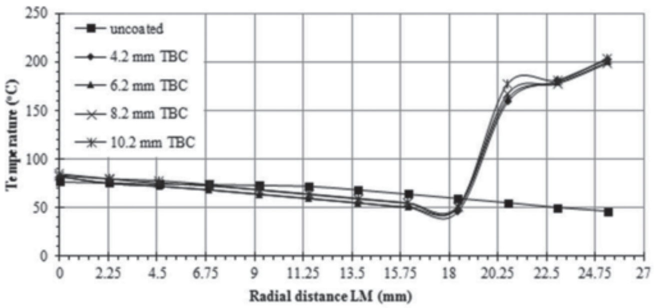

Fig.4(b) Top surface temperature distribution with coating width

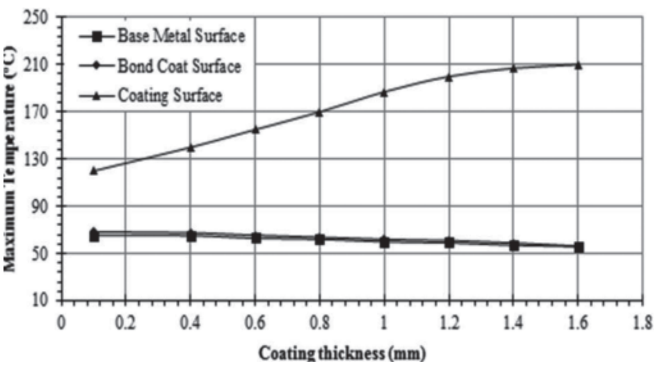

Fig.5 Maximum temperature variation as a function of coating thickness

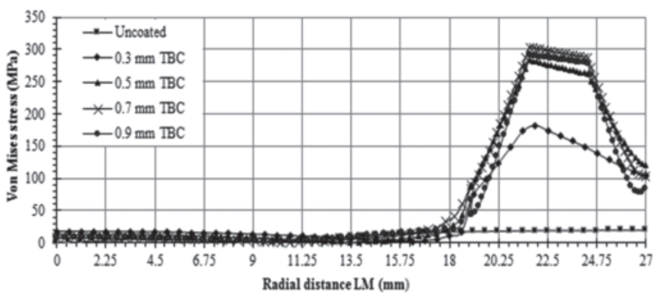

Fig.6 Normal stress variation as a function of coating thickness for top surface

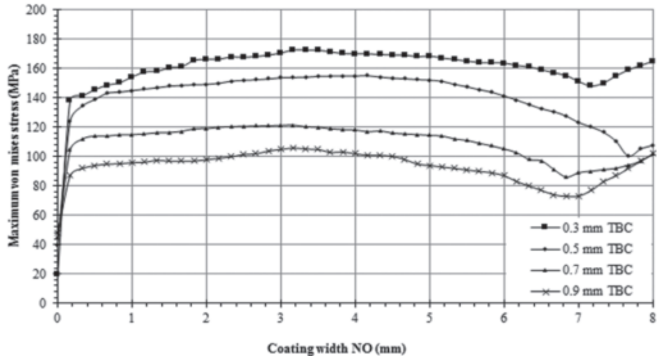

Fig.7 Normal stress variation as a function of coating thickness at bond coat

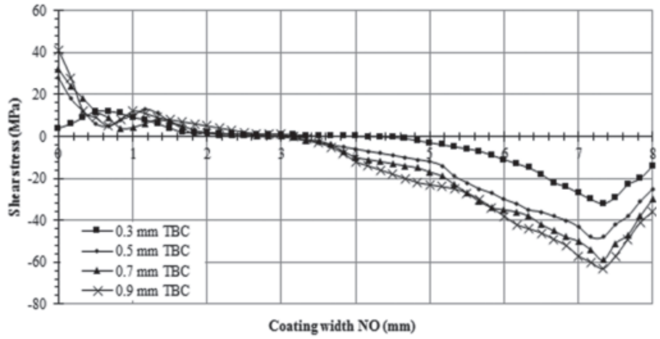

Fig.8 Shear stress variation as a function of coating thickness at bond coat surface

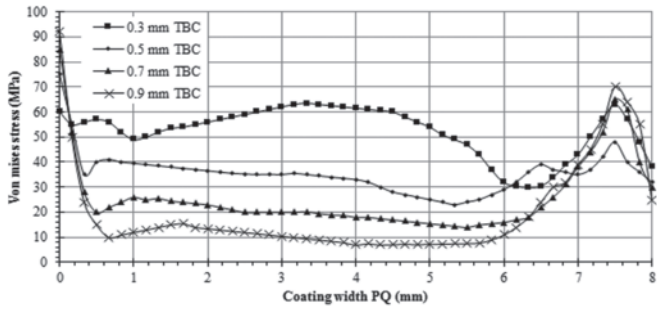

Fig.9 Normal stress variation as a function of coating thickness for substrate surface

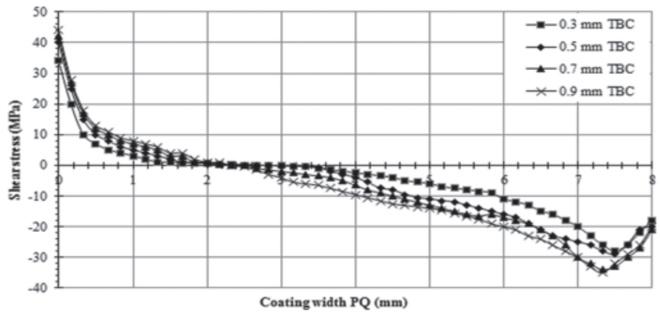

Fig.10 Shear stress variation as a function of coating thickness for substrate surface

surface but the magnitude of the bond low stress is higher than that of bond coat. Hence, on edges, surface cracks would exist.

Figs.11 and 12, represents the variation of normal and shear stress with coating thickness on the ceramic coating, bond coat and substrate surface. It is observed that Von Mises stress is function of coating thickness and its value decreases with the increase in coating thickness. Normal

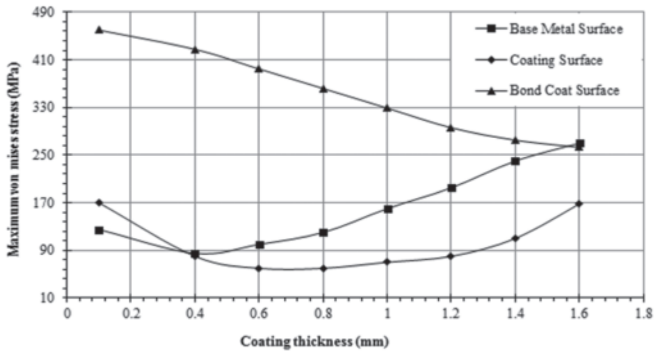

Fig.11 Maximum normal stress variation with coating thickness

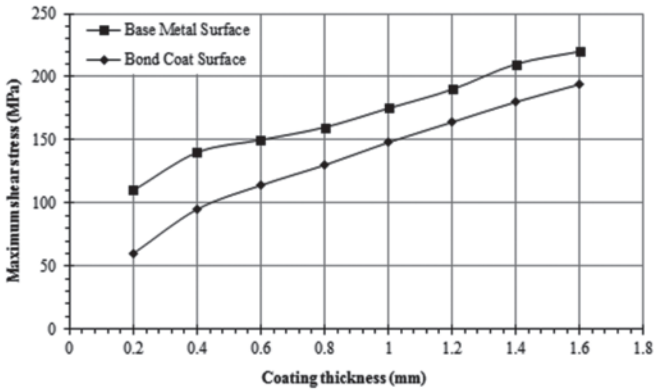

Fig.12 Maximum shear stress variation with coating thickness for interfaces

stresses caused the surface crack in the middle of the bottom surface of ceramic coating and spalling of coating. The cracks shifted towards the inner edge of coating with the increase in coating thickness. Maximum normal stress also causes spalling of the ceramic top coat from the bond coat occurs on the bond coat surface. Shear stresses may cause the lateral cracks. It was observed that maximum shear stress value increases constantly with the coating thickness at the interface of bond coat and substrate. The substrate coated inner region experienced the maximum value of shear stress and the value of shear stress is maximum at the substrate interface in comparison with bond coat.

Conclusions

From numerical analysis, it was observed that coating thickness affects the temperature distribution on the surface of uncoated and coated piston. For ceramic coated piston, development of higher surface temperature distribution was observed in comparison with uncoated piston. From the above analysis, we can conclude the following:

- Maximum value of temperature was found at the center of uncoated piston top surface and for partially coated piston, the maximum value of temperature moves out to the skirt region. The surface of coated piston has experienced higher value of temperature in comparison with uncoated piston surface. For all models, within coated region the rate of increase of temperature is very high for different coating thickness. It was observed that the surface temperature is unaffected by the variation in coating width for same coating thickness.
- From thermal analysis, it was found that coating on the piston caused the increase in temperature for those sections, which are close to crevice and wall quenching regions. Further this rise in temperature caused the increase in air fuel mixture temperature in those sections and hence near the entrance of clearance, the unburned charge oxidation increases. Also with rise in temperature, the emission of carbon monoxide decreases due to the reliance of CO oxidation reaction on temperature.
- It was observed that the maximum stress is a function of coating thickness. These stresses caused the surface cracking, spalling. Surface cracks and spalling are generally caused by the normal stresses. The cracks takes place at the middle of the bottom surface of the ceramic coating width in radial direction. The cracks moves towards the inner edge of coating with the increase in coating thickness. Spalling of the ceramic top coat from the bond coat due to maximum normal stresses occurs on the bond coat interface. The Von Misses stress decreases with increasing coating thickness. The lateral cracks are caused by the shear stress and there values increase with coating thickness and reaches to a maximum value at the inner edge of the coated region at the interface of substrate.

References

1. Assanis, D. and Mathur, T. (1990): "The Effect of Thin Ceramic Coatings on Spark-Ignition Engine Performance," *SAE Technical Paper 900903*, 1990, doi: 10.4271/900903.
2. Buyukkaya, E. (1997), "Effects of thermal barrier coating on a turbocharged diesel engine exhaust emissions," Sakarya University, Mechanical Engineering Department, Ph D. thesis, Institute of Sciences and Technology, Turkey, 1997.
3. Buyukkaya, E. (2008): *Surf. Coat. Technol. 202* (2008) 3856.
4. Heiwowski, T. and Weronski, A (2002): "The effect of thermal barrier coatings on diesel engine performance" *Vacuum*, Volume 65, Issues 3-4, 27 May 2002, Pages 427-432.
5. Buyukkaya, E. and Cerit, M. (2007): *Surf. Coat. Technol. 202* (2007) 398.
6. Beardsley, M. B., Happoldt, P. G., Kelley, K. C., Rejda, E. F. and Socie, D. F. (1999): "Thermal Barrier Coatings for Low Emission, High Efficiency Diesel Engine Applications," 1999 *SAE Paper Number: 2255*.
7. Vittal, Manohar, Borek, Jeffrey, Boehman, Dr. Andre L.

and Okrent, D. A. (1997): "The Influence of Thermal Barrier Coatings on the Composition of Diesel Particulate Emissions," 1997. *SAE Paper Number: 970799*.

8. Winkler, Matthew F. and Parker, Daniel W. (1993): "Ceramic Thermal Barrier Coatings Provide Advanced Diesel Emissions Control and Improved Management of Combustion-Exhaust System Temperatures," 1993. *SAE Paper Number: 931106*.
9. Kahl, W. K. (1993): "Thermal Barrier Effects on Performance and Emissions of a Methanol Fueled Dl Engine," 1993. *SAE Paper Number: 892163*.
10. Gilbert, A., Kokiniand, K. and Sankarasubramanian, S. (2008): *Surf. Coat. Technol. 203* (2008) 91.
11. Gilbert, A., Kokiniand, K. and Sankarasubramanian, S. (2008): *Surf. Coat. Technol. 202* (2008) 2152.
12. Muchai, Jesse G., Kelkar, Ajit D., Klett, David E. and Jagannathan, Sankar (2002): Thermal-Mechanical Effects of Ceramic Thermal Barrier Coatings on Diesel Engine Piston, Mat. Res. Soc. Symp. Proc., Vol. 697, Materials Research Society, 2002.
13. Cerit, M., Ayhan, V., Parlak, A. and Yasar, H. (2011): *Appl. Therm. Eng.* 31 (2–3) (2011) 336.
14. Prasad, Ravindra and Samria, N. K. (1990): *Comput. Struct.* 34 (5) (1990) 765.
15. Parlak, A. and Ayhan, V. (2007): *J. Energy Inst.* 80 (4) (2007).
16. Marr, Michael Anderson (2009): An Investigation of Metal and Ceramic Thermal Barrier Coatings in a Spark-Ignition Engine, M.S thesis, Mechanical and Industrial Engineering, University of Toronto, 2009.
17. Martin, W., Patrik, S., Christian, S., Anna, M. F. and Norbert, H. (2005): *Atmos. Environ.* 39 (2005) 2433.
18. Poola, Ramesh B., Nagalingam, B. and Gopalakrishnan, K. V. (1994): "Performance of Thin Ceramic Coated Combustion Chamber with Gasoline and Methanol as Fuels in a Two-Stroke SI Engine," 1994. *SAE Paper Number: 941911*.
19. Esfahanian, V., Javaheri, A. and Ghaffarpour, M. (2006): *Appl. Therm. Eng.* 26 (2006) 277.
20. Hohenberg, G. F. (1979): "Advanced Approaches for Heat Transfer Calculations," 1979. SAE Technical. Paper, No. 790825.
21. Cerit, Muhammet (2011): "Thermo mechanical analysis of a partially ceramic coated piston used in an SI engine" *Surface & Coatings Technology* 205 (2011) 3499-3505.
22. Muchai, Jesse G., Kelkar, Ajit D., Klett, David E. and Jagannathan, Sankar (2002): Thermal– Mechanical Effects of Ceramic Thermal Barrier Coatings on Diesel Engine Piston, Mat. Res. Soc. Symp. Proc., Vol. 697, Materials Research Society, 2002.

Printed by Pradip Kumar Chanda at The Indian Press Pvt. Ltd. 93A Lenin Sarani, Kolkata 700 013 and published by him for Books & Journals Pvt. Ltd. from 6/2 Madan Street, Kolkata 700 072.